Synthesis of Y_2O_3:Eu Phosphor Nanoparticles by Flame Spray Pyrolysis

Xiao Qin[*], Yiguang Ju[*], Stefan Bernhard[**] and Nan Yao[***]

[*]Dept. of Mech. & Aerospace Engineering, Princeton University, Princeton, NJ 08544
[**]Dept. of Chemistry, Princeton University, Princeton, NJ 08544
[***]Princeton Materials Institute, Princeton University, Princeton, NJ 08544

ABSTRACT

Nanoscale europium doped yttrium oxide (Y_2O_3:Eu) particles synthesized by flame spray pyrolysis method and the effect of precursor solution on particle size, morphology and photoluminescence intensity was studied. The structure and morphology of the as-prepared particles were examined using scanning electron microscopy (SEM). The photoluminescence (PL) intensity was measured by a spectrophotometer. Compared with previous report, SEM shows fine and smooth structure for particles prepared from ethanol alcohol as precursor solution. The particle size can be controlled by varying precursor concentration, flame temperature and residence time. Upon excitation with 355 nm UV light, the particles show red emission and the PL intensity of particles using ethanol is 30% stronger than those using water as precursor solution. Annealing particles at 1200°C can convert the monoclinic phase into cubic phase. The concentration quenching limit of the prepared particles was 18% mol Eu.

Keywords: nanoparticles, europium, yttrium oxide, flame spray pyrolysis, photoluminescence, quenching.

1. INTRODUCTION

Nanoparticles have become a research focus in terms of both their fundamental and technological importance, especially in the case of luminescent materials because of a quantum confinement effect which leads to novel optoelectronic properties. It was found that the emission lifetime, luminescence quantum efficiency, and concentration quenching depend strongly on the size in the nanometer range [1-4]. Nanoparticles have great potential for use in applications in electronic, chemical and mechanical industries, as well as technologies which include superconductors, catalyst, drug carriers, sensors, materials, pigment, structural materials, and so on [5].

Europium doped yttrium oxide (Y_2O_3:Eu) is a typical red phosphor that is widely used in optical displays and lighting applications. The better quality of a high resolution display requires smaller size phosphors and nanosized Y_2O_3:Eu phosphor has significant promise in displays due to the quantum efficiency increase of doped nanocrystals [6,7]. Various methods, such as solid state reactions, sol–gel techniques [8], hydroxide precipitation [9], hydrothermal synthesis [10], laser-heated evaporation [11], spray pyrolysis [12], and combustion synthesis [13] were used to prepare nanostructured Y_2O_3:Eu phosphors.

Flame spray pyrolysis (FSP), also called liquid flame spray (LFS), is a promising particle synthesis method because it can employ a wide range of precursors for synthesis of a broad spectrum of functional nanoparticles [14-16]. Using FSP method, Kang et al. [17] prepared nonagglomerated Y_2O_3:Eu phosphor particles of size on the order of 1 μm and had spherical and dense morphology. Their as-prepared particles had a monoclinic phase with small impurities of the cubic phase. Tanner and Wong [18] synthesized Y_2O_3:Eu nanoparticles using preformed sol, conventional spray pyrolysis and flame spray pyrolysis methods and compared the luminescence properties of the powders prepared by these three methods. Chang et al. [19] fabricated cubic nanocrystalline Y_2O_3:Eu phosphors using FSP method without any post-heat treatments.

In flame spray pyrolysis, the precursor composition is a key parameter to control the particle properties. The precursor releases from the droplet and its evaporation, decomposition, and gas phase reaction plays an important role in the formation of the final product. To the best of our knowledge, there's no report on the effect of precursor composition on the synthesis of Y_2O_3:Eu phosphorous nanoparticles in flame spray pyrolysis. Our objective of the present work is to synthesize Y_2O_3:Eu nanoparticles by using FSP method and study the effect of precursor composition on the product properties.

2. EXPERIMENTAL METHOD

Figure 1 shows the schematic of the flame spray pyrolysis system. The system consisted of a spray generator, a coflow burner, a quartz reactor, particle collection filters and a vacuum pump. An ultrasonic spray generator operating at 1.7 MHz was used to generate fine spray droplets which were then carried into the flame by nitrogen gas though a 5.3 mm central pipe. The flame nozzle consisted of three concentric pipes. A Methane and oxygen nonpremixed flame was used and an air coflow was also introduced into the reactor. By varying the flow rate of fuel, oxidant and coflow air, the flame temperature and particle residence time can be controlled. The temperature measurements along the centerline employed uncoated 100 μm diameter R-type wire thermocouples with a junction

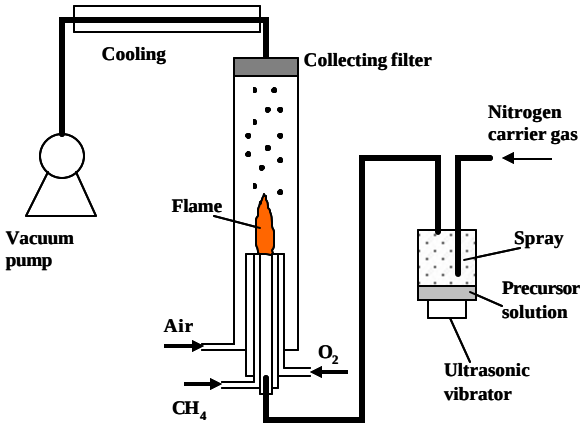

Figure 1: Schematic of experimental setup.

bead diameter of 350±30 μm and were corrected for radiation heat losses.

To study the effect of precursor solution on particle properties, ethanol and water were selected as solvent. The starting precursor solution was prepared by dissolving yttrium and europium nitrate, i.e. $Y(NO_3)_3 \cdot 6H_2O$ and $Eu(NO_3)_3 \cdot 6H_2O$, in pure water or ethanol alcohol. The overall concentration was varied from 0.1 to 0.001 M and the doping concentration of europium varied from 3 to 21 mol% with respect to yttrium. The particles, which were collected using a micron glassfiber filter (Whatmann GF/F) located 30 cm above the flame. The structure and morphology of the as-prepared particles were examined using a Philips XL30 FEG-SEM scanning electron microscope. The photoluminescence intensity of the particles excited by UV light is measured by a spectrophotometer (Fluorolog, Jobin Yvon Group) with a xenon lamp of 150 W.

3. RESULTS AND DISCUSSION

Figure 2 shows SEM photographs of as-prepared Y_2O_3:Eu particles by flame spray pyrolysis using distilled water (Fig. 2a and 2b) and ethanol (Figs. 2c and 2d) as precursor solvent at different overall concentrations. The europium doping concentration was 6 mol% with respect to yttrium for all cases. The effect of precursor solution on particle morphology and size can be clearly seen from these images. The particles made from aqueous solution (c.f. Fig. 2a and 2b) have a fuzzy structure on the surface and broader size distribution. On the other hand, the particles using ethanol as precursor solution (Fig. 2c and 2d) exhibit smoother surface structure and improved homogeneity in distribution. Regardless of the overall concentration and precursor solution type, the particles are generally non-aggregated and have a spherical morphology. Table 1 lists the average particle size, geometric standard deviation calculated from the SEM images at different precursor concentration with a fixed doped Eu concentration of 6 mol% with respect to yttrium. The average size has been determined by measuring the

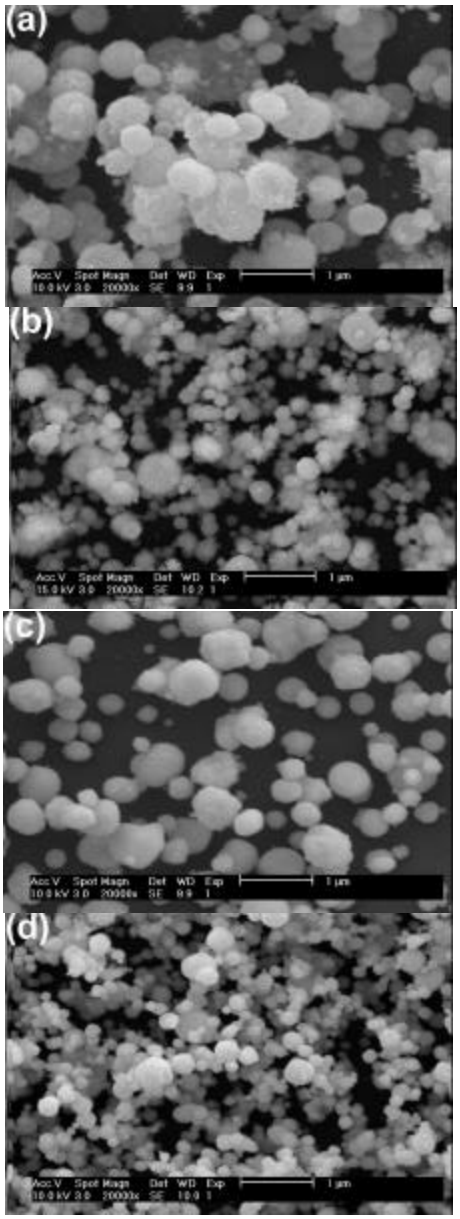

Figure 2: SEM photographs of Y_2O_3:Eu particles prepared from (a) distilled water solution, 0.1 M; (b) distilled water solution, 0.01 M; (c) ethanol solution, 0.1 M; (d) ethanol solution, 0.01 M.

diameters of 500 particles from SEM images. It is seen that particles prepared from ethanol solution has smaller average diameter than those from water solution of the same concentration. The average diameter of the particles varied from 114 nm to 412 nm when the ethanol precursor solution concentration increased from 0.001 M to 0.1 M (c.f. cases 4, 6 and 8) which shows that the particle size can be controlled by changing the overall concentration.

The differences in particle morphology and size distribution when using ethanol and water as precursor solvent arise from the different physical properties between ethanol and water. Ethanol has a lower boiling point and

Table 1: The particle average diameter, geometric standard deviation of the as-prepared particles and flame temperature

case	Precursor concentration (M)	Precursor type	Particle average diameter (nm)	Geometric standard deviation	Flame temperature* (K)
1(Fig.2a)	0.1	Water	535	1.20	1721
2	0.1	Water	498	1.20	2030
3(Fig.2b)	0.01	Water	192	1.31	1720
4(Fig.2c)	0.1	Ethanol	412	1.14	2030
5	0.01	Ethanol	185	1.07	1800
6(Fig.2d)	0.01	Ethanol	198	1.10	2040
7	0.01	Ethanol	214	1.09	2260
8	0.001	Ethanol	114	1.07	2050

*At centerline location of 20 cm above the burner exit.

enthalpy of evaporation (78 °C and 838 kJ/kg) than water (100 °C and 2258 kJ/kg). And more importantly, ethanol is a fuel that directly reacts and release heat in the flame instead of take away heat from the flame when using water. To investigate the effect of precursor solution on flames, the temperature profiles along the centerline for the flames corresponding to Figs. 2a and 2c were measured by thermocouples and shown in Fig. 3. In the measurements, methane, oxygen, nitrogen and coflow air flow rates were kept constant for the two cases. It should be mentioned that near the core of the methane-oxygen flame (<10 cm) the flame temperature is so high that the thermocouple immediately breaks; therefore, only data above 10 cm were taken. Along the centerline, the temperature of the flame using ethanol as precursor solution is consistently 200 K higher than the flame using water. It is known that in flame spray pyrolysis higher flame temperature increases particle sintering and agglomerating, which is not the case in our observation in Fig. 2. This suggests that not only flame temperature but other parameters, such as evaporation, gas phase reaction, nucleation, etc. may also affect particle size and morphology. The faster evaporation of ethanol droplets when passing the preheating zone of the flame produces smaller droplets that determine the final particle size. In the aqueous solution, the presence of water droplets or vapor in the reaction zone results in larger particles. Limaye and Helble [20] observed similar effect of precursor and solvent on the morphology of zirconia nanoparticles produced by combustion aerosol synthesis.

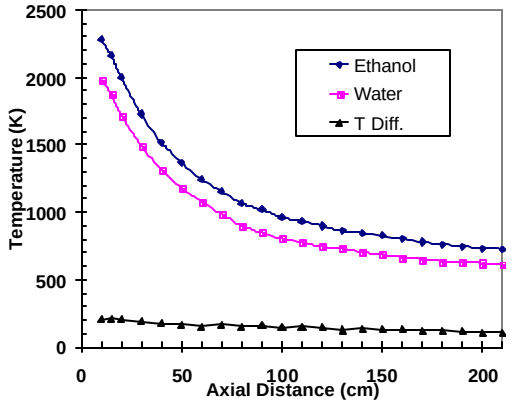

Figure 3: Temperature distribution along the centerline of the flames using different precursor solutions.

By only increasing the methane flow rate of the flame in Fig. 2a, the same temperature distribution as that in Fig. 2b was achieved. The mean particle size decreased to 498 nm from 535 nm (cases 1 and 2 in Table 1), but still larger than that from ethanol flame (412 nm). The increase of flame temperature helped to evaporate the precursor droplet and produced smaller particles. On the other hand, we kept the oxygen, nitrogen and air flow rates constant and adjusted the methane flow rate for the flame in Fig. 2d to achieve three different flame temperatures. As listed in Table 1 (cases 5-7), the temperature at the centerline location of 20 cm above the burner exit is 1800 K, 2040 K, and 2260 K, respectively. The average particle size is 185, 198 and 214 nm, respectively. The flame length for case 7 is about 10 cm longer than in case 5. At higher flame temperatures the sintering and coagulation rates increase and enhance the formation of larger particles. The longer flame length increases the residence time of particles and gives more time for the particles to grow.

Figure 4 shows the photoluminescence spectra of Y_2O_3:Eu nanoparticles exited by UV light at 355 nm. The spectra of the particles prepared from water solution (Fig.

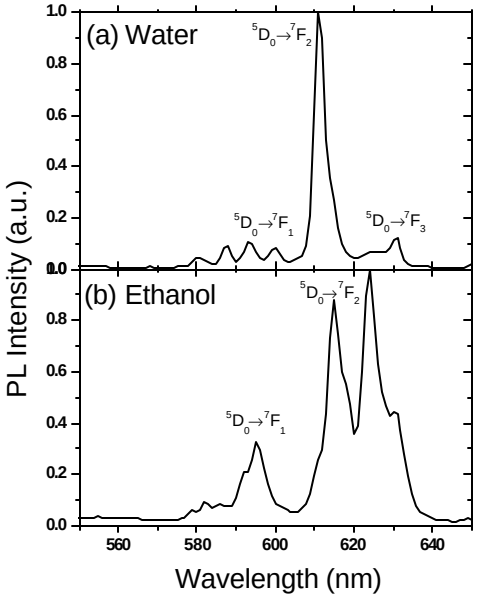

Figure 4: Photoluminescence spectra of Y_2O_3:Eu nanoparticles exited at 355 nm UV light with (a) water (b) ethanol as precursor solution.

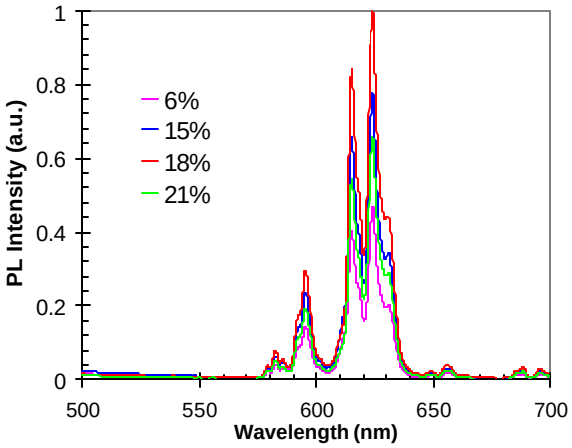

Figure 5: Photoluminescence spectra of Y_2O_3:Eu nanoparticles at different doping concentration (Eu mol% with respect to Y).

4a) shows a typical Y_2O_3:Eu^{3+} emission spectrum, which is described by the well known $^5D_0$? ^7F_J (J = 0, 1, 2 …) line emissions of the Eu^{3+} ions with the strongest emission for J = 2 at 611 nm. However, the PL spectrum of the particles made from ethanol solution shows a split peak at 615 nm and 624 nm, respectively. This is due to the nonuniformity of the yttrium oxide crystalline structure, which exhibits both monoclinic and cubic phase. By annealing the sample at 1200 °C for 2 hours can transform the monoclinic phase into cubic phase and results in a single peak PL spectrum. The intensity in Fig. 4b is 30% higher than that in Fig. 4a. Further study on the annealing effect is undergoing.

Figure 5 shows the effect of europium doping concentration on the photoluminescence intensity of as-prepared Y_2O_3:Eu nanoparticles using ethanol precursor solution. Different from the reported value of 6% for bulk materials, the quenching concentration is 18% for particles prepared in this study. This is in agreement with the result of Zhang et al. [21] for their 5nm Y_2O_3:Eu crystalline prepared by solid state reaction method. Tao et al. [13] reported a value of 14% and argued that the increase of the quenching concentration could be described as the delay of the energy transfer due to the interface effects of the nanoscale materials. It can be concluded from the previous researches that the quenching concentration increases from 6% to 18 mol% when the crystallite size decrease from 3 µm to 5 nm. XRD examination will be performed on our nanoparticles to obtain the crystallite size in this study.

4. CONCLUSIONS

Europium doped yttrium oxide (Y_2O_3:Eu) phosphor nanoparticles were synthesized by flame spray pyrolysis method and the effect of precursor solution on particle size, morphology and photoluminescence intensity was studied. Compared with previous report, SEM shows fine and smooth structure for particles prepared from ethanol alcohol as precursor solution. The particle size can be controlled by varying precursor concentration, flame temperature and residence time. Upon excitation with 355 nm light, the particles show red emission and the PL intensity of particles using ethanol is 30% stronger than those using water as precursor solution. Annealing particles at 1200°C can convert the monoclinic phase into cubic phase. The concentration quenching limit was also increased to 18% mol Eu. It is expected that these particles will be useful in developing emission field or high resolution displays and be used as markers in biomedical research.

ACKNOWLEDGEMENTS

This work was supported by National Science Foundation grant (0303947).

REFERENCES

[1] C. Suryanarayana. *Int. Mater. Rev.* **40** (1995) 41.
[2] F.E. Kruis, H. Fissan and A. Peled. *J. Aerosol Sci.* **29** (1998) 511.
[3] S. Sun and C.B. Murray. *J. Appl. Phys.* **85** (1999) 4325.
[4] T. Hase, T. Kano, E. Nakazawa and H. Yamamoto. *Adv. Electron. Phys.* **79** (1990) 271.
[5] G. Blasse and B. C. Grabmaier, *Luminescent Materials*, Berlin, Springer, 1994.
[6] R. N. Bharava, D. Gallager, X. Hong and A. Nurmikko. *Phys. Rev. Lett.* **72** (1994) 416.
[7] T. Igarashi, M. Ihara, T. Kusunoki, K. Ohno, T. Isobe and M. Senna. *Appl. Phys. Lett.* **76** (2000) 1549.
[8] C. N. R. Rao. *Mater. Sci. Engng. B* **18** (1993) 1.
[9] K. M. Kinsman, J. Mckittrick, E. Sluzky and K. Hesse. *J. Am. Ceram. Soc.* **77** 11 (1994) 2866.
[10] C. D. Veitch. *J. Mater. Sci.* **26** (1991) 6527.
[11] H. Eilers, B. M. Tissue, *Chem. Phys. Lett.* **251** (1996) 74.
[12] Y. C. Kang, H. S. Roh and S. B. Park. *Adv. Mater.* **12** (2000) 451.
[13] Y. Tao, G. W. Zhao, W. P. Zhang and S. D. Xia. *Mater. Res. Bull.* **32** (1997) 501.
[14] S. E. Pratsinis, *Prog. Energy Combust. Sci.* **24** (1998) 197.
[15] H. K. Kammler, L. Madler and S. E. Pratsinis, *Chem. Eng. Technol.* **24** (2001) 6.
[16] L. Mädler, H. K. Kammler, R. Mueller, and S. E. Pratsinis, *J. Aerosol Sci.*, **33** (2002) 369
[17] Y. C. Kang, D. J. Seo, S. B. Park and H. D. Park, *Jpn. J. Appl. Phys.* **40** (2001) 4083.
[18] P. A. Tanner and K. L. Wong, *J. Phys. Chem. B* **108** (2004) 136.
[19] H. Chang, I. W. Lenggoro, K. Okuyama, and T. O. Kim, *Jpn. J. Appl. Phys.* **43** (2004) 3535.
[20] A. U. Limaye and J. J. Helble, *J. Am. Ceram. Soc.* **86** (2003) 273.
[21] W.-W. Zhang, W.-P. Zhang, P.-B. Xie, M. Y. H.-T. Chen, L. Jing, Y.-S. Zhang, L.-R. Lou, and S.-D. Xia, *J. Colloid Interface. Sci.* **262** (2003) 588.